Palladium-polyaniline type composite polymers: Using catalysis as a monitor of palladium location

Kaushik Mallick[a], Kartick Mondal[b], Michael J. Witcomb[c], Stefania M. Scalzullo[b], Tshifiwa Maphala[b] and Michael S. Scurrell[b*]

The location of nanosized (2–4 nm) palladium particles in two palladium–polyaniline-based composites, synthesized by the redox coupling route using monomer and palladium(II) acetate, have been revealed using ethene hydrogenation as a heterogeneously catalysed reaction, together with differential scanning calorimetry. The two palladium composites were synthesized using *m*-aminobenzoic acid (ABA) or *o*-phenylenediamine (PDA), leading to Pd-PABA or Pd-PPDA, respectively. The temperature sensitivity of catalytic activity related to the polymer melting temperature, as revealed by DSC, assists in understanding the location of the palladium particles. The structures of the metal–polymer composite at the micrometre and nanometre levels are revealed using scanning and transmission electron microscopy, respectively.

Introduction

Semiconducting polymers are a special class of organic compounds.[1,2] Like inorganic semiconductors, they also have holes, an electron conduction layer and a band gap. Organic semiconductors can also be doped as a means of modifying structure and behaviour. The polymer polyaniline has been extensively studied due largely to its environmental stability, controllable electrical conductivity and interesting redox properties associated with chain nitrogen.[1,3–5] Potential applications of polyaniline include lightweight batteries, microelectronics, electrochromic displays, electromagnetic shielding and chemical and biochemical sensors.[4,6]

Polyaniline has the general formula $[(–B–NH–B–NH–)\ y\ (–B–N=Q=N–)(1 – y)]x$. The redox states can vary from that of the fully oxidized *pernigraniline* ($y = 0$) to that of the fully reduced *leucoemeraldine* ($y = 1$). The 50% oxidized polymer has been termed *emeraldine* ($y = 0.5$), while the 75% oxidized polymer is named *nigraniline* ($y = 0.75$).

The synthesis of polyaniline systems has been documented and various morphologies can result, ranging from nanofibres,[7,8] nanospheres[4] and nanotubes.[9] Four general methods for the synthesis of metal–polymer composites may be distinguished.[10] Of these, the monomer + metal salt approach is particularly interesting in that, if the salt is readily reducible the composite is actually produced by a redox coupling of the polymerization (oxidation) and metal formation (reduction). The method has the potential of offering a very intimate contact between polymer and metallic particles as these are produced simultaneously from molecular precursors. Further, the growing polymer acts as a break on metal particle growth, so that the formation of nanosized metallic particles embedded in a polymer network can readily be achieved. The approach has been illustrated by the synthesis of various gold-,[4,11,12] palladium-[7,13–15] and copper-[8,16] polyaniline composites, starting with Au(III), Pd(II) or Cu(II) salts, respectively. The monomer may be aniline itself [4,11,17,18] or a substituted aniline, such as 3, 5-dimethylaniline,[7,16] *o*-toluidine,[8] *o*-phenylenediamine,[12,13] *o*-aminophenol,[14] or *o*-methoxyaniline.[15] Work on gold–polymer composites[19] and palladium–polymer composites[20] have recently been reviewed. The essential features of materials synthesized by the redox coupled molecular synthesis approach are nanosized metal particles, as small as *c.* 2–3 nm,[15] composited with a polymer matrix, the morphology of which is controllable depending on the chemical nature of the monomer used. Given the orientation of the polymerization of aniline derivatives, the use of *ortho*- or *meta*-substituted anilines is of particular interest.

In most studies the nanometal particles are clearly identifiable (unless very small) using electron microscopy, essentially transmission electron microscopy (TEM) coupled with energy dispersive X-ray spectroscopy (EDX) data. Electron energy loss spectroscopy (EELS) can also be useful.[15] However, the precise location of the metal particles and their physical environment is not always clear from such structural studies alone. For example, it is not known if the metal particles are physically embedded in the polymer matrix or whether they are exposed at the surface of the composite, a factor which has important consequences for making, for example, electrical and/or chemical contact between metal and the external environment, for instance, an electrical contact or a molecular contact with a chemical substance in the case of the composite being used as a sensor. We have attempted to reveal something of the surface exposure of the metal particles in nanometal composites by using a heterogeneous catalytic test reaction. The approach is illustrated by a study of the ability of palladium contained within a palladium–poly(*m*-aminobenzoic acid) composite (Pd-PABA) or a palladium–poly(*o*-phenylenediamine) (Pd-PPDA) composite to exhibit reactivity in the catalytic hydrogenation of ethene.

This simple, easily monitored reaction will clearly take place in these systems under mild conditions only if exposed palladium atoms are available to effect contact between ethene and hydrogen arriving at the surface of the composite from the gas phase. It might be envisaged that the approach can be made even more sophisticated by choosing a more complex catalytic reaction, in which, for example, more than one product could be formed. Selectivity as well as activity could then be monitored and subtle changes in palladium surface chemistry revealed. For the present purpose, however, we confine ourselves to using catalytic activity alone as a means of monitoring palladium surface exposure.

Experimental

The monomers *m*-aminobenzoic acid and *o*-phenylenediamine were obtained from BDH, methanol and toluene from Merck, and palladium acetate was obtained from NextChimica and dissolved in toluene as a stock solution (2×10^{-2} mol dm^{-3}).

The *m*-aminobenzoic acid (1.02 g) was dissolved in methanol (15 cm^3) at room temperature and stirred continuously until a pale brown-purple solution was obtained (after *c.* 20 min). The palladium stock solution (6 cm^3) was added dropwise to the monomer solution, with continuous stirring. The emulsion became more viscous and was stirred for a further 90 min. The solvent was then allowed to evaporate slowly at room temperature over a period of 48 h. The dried solid metal–polymer composite Pd-PABA was obtained and was characterized using TEM, SEM, IR, UV-vis, DSC, and XRD. For SEM, images were obtained by using a JEOL

[a]Advanced Materials Division, Mintek, Private Bag X3015, Randburg 2125, South Africa.
[b]Molecular Sciences Institute, School of Chemistry, University of the Witwatersrand, Private Bag 3, WITS 2050, South Africa.
[c]Microscopy and Microanalysis Unit, University of the Witwatersrand.
*Author for correspondence. E-mail: michael.scurrell@wits.ac.za

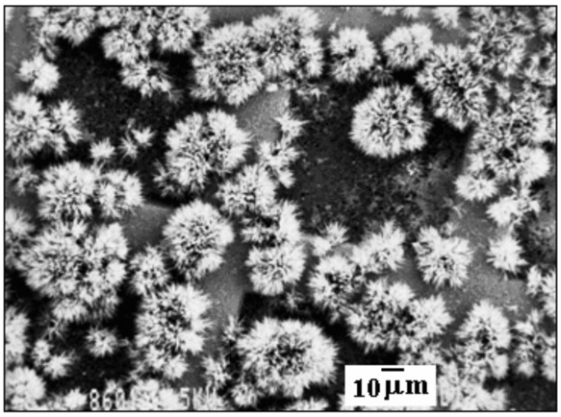

Fig. 1. SEM image obtained from as-synthesized Pd-PABA.

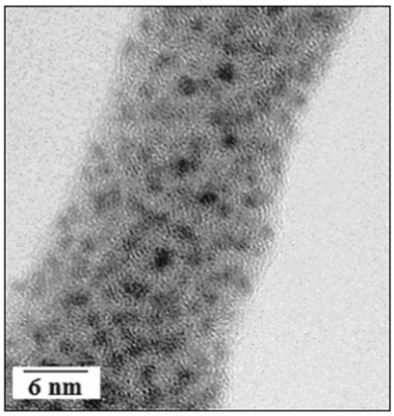

Fig. 2. TEM image showing palladium nanoparticles in as-synthesized Pd-PABA.

JSM-840 instrument with an accelerating voltage of 20 kV in the magnification range 450–19 000×. TEM studies were carried out at an accelerating voltage of 197 kV using a Philips CM200 microscope. An ultrathin windowed energy-dispersive X-ray spectrometer (EDX) and a Gatan Imaging Filter (GIF) attached to the TEM were used to effect chemical mapping of the samples. DSC data were recorded using a Perkin-Elmer Pyris DTA 7 with small (*c.* 7 mg) samples in aluminum pans and applying a temperature ramp rate of 10°C min^{-1} in the range 30–200°C.

For the synthesis of the Pd-PPDA material, *o*-phenylenediamine (120 mg) was dissolved in toluene and the palladium stock solution (3 cm^3) added with continuous stirring. Structural characterization was carried out as for Pd-PABA. Both composites were also tested for the catalytic hydrogenation of ethylene. For the latter test, the solid was placed in a glass fixed-bed reactor, pretreated in flowing hydrogen at 70°C for 60 min. Thereafter a flow of ethene and hydrogen (H_2/C_2H_4 = 3.05 mol mol^{-1}, flow rate = 71 000 $(Ncm)^3$ g^{-1} h^{-1}) at a total pressure of 0.84 kPa was passed through the reactor and the exit gas stream analysed (for ethene and ethane) using a gas chromatograph fitted with a flame ionization detector. Catalytic activity was monitored over the temperature range 80–170°C for Pd-PABA and 80–100°C for Pd-PPDA.

Results and discussion

Pd-PABA composite

SEM revealed that the composite comprised flower-shaped polymer material, with individual 'flowers' having diameters in the range 10–40 μm (Fig. 1). TEM revealed the presence of palladium particles in the size range 2–4 nm (Fig. 2). Corroboration was obtained by means of XRD. Line broadening analysis using the Scherrer equation suggested that the mean Pd diameter was close to 2.5 nm. DSC examination revealed a pronounced endotherm at approximately 179°C, which was attributed to the melting of the polymer matrix. Catalytic activity for ethylene hydrogenation (and due to the presence of the palladium particles) was a maximum at a reaction temperature of around 130°C (Fig. 3), a temperature far below the melting point. In fact at 170°C, catalytic activity was relatively low. Detailed time-on-stream analysis for ethylene hydrogenation at 130°C revealed a steady slow increase in activity over a period of up to 1400 min (Fig. 4). After reaction, EM analysis revealed that the 'flower' structures had disappeared and that the polymer structure was far less defined at the micrometre level. The palladium particles were found to have grown to diameters in the range 5–15 nm (Fig. 5). The initially small palladium particles of 2–4 nm may well be expected to demonstrate catalytic properties for ethene hydrogenation not very different from those of larger palladium particles,[20] since deviations from bulk properties can be expected at particle diameters somewhat lower than 2 nm.[21] However, it may be that some very small (*c.* 1 nm diameter or below) palladium particles, present in the as-synthesized Pd-PABA, but not readily observable in the TEM images, grow during reaction, e.g.

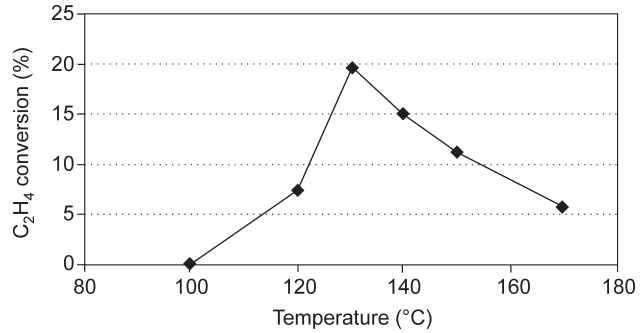

Fig. 3. Ethene hydrogenation activity of Pd-PABA as a function of reaction temperature (for the catalytic reaction conditions used see text).

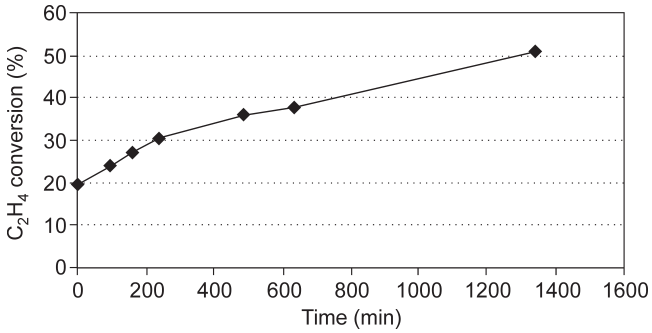

Fig. 4. Ethene hydrogenation activity of Pd-PABA as a function of time-on-stream for reaction at 130°C (for the catalytic reaction conditions used see text).

at 130°C, and gradually contribute to hydrogenation activity. This would explain the gradual upward incline depicted in Fig. 4.

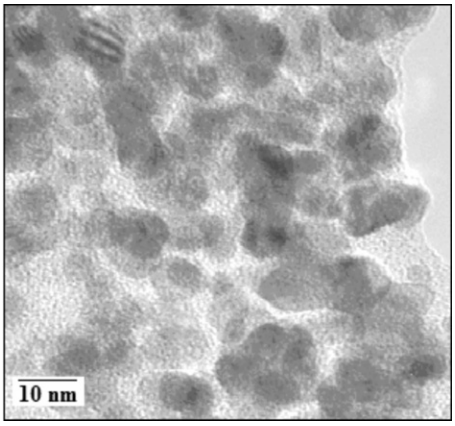

Fig. 5. TEM image of Pd-PABA after use in ethene hydrogenation runs at up to 170°C.

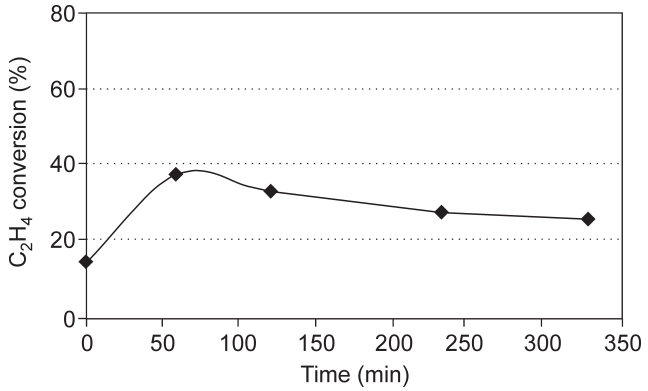

Fig. 6. Ethene hydrogenation activity of Pd-PPDA as a function of time-on-stream for reaction at 100°C.

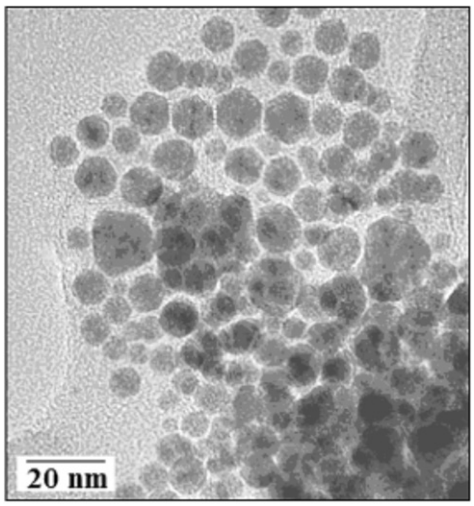

Fig. 7. TEM image of Pd-PPDA after use in ethene hydrogenation runs at 100°C.

Pd-PPDA composite

No regular polymer shape was revealed by SEM. TEM showed that the palladium metal particles possessed diameters in the range 2–3 nm, similar to those found in Pd-PABA. DSC indicated that the metal–polymer composite melted at 10°C, a much lower temperature than that seen for Pd-PABA. Significant catalytic activity was seen only at a reaction temperature of 100°C, and little or no ethylene hydrogenation was observed at 80 or 90°C. At 100°C, time-on-stream behaviour clearly showed that catalytic activity reached a broad maximum after about 65 min on stream and then fell steadily (Fig. 6). TEM data revealed that the palladium particles had now grown to a diameter of about 20–25 nm (Fig. 7). It is clear that in comparison with the Pd-PABA system, the Pd-PPDA exhibits an onset of ethene hydrogenation activity at a lower relative temperature, but such activity develops only at the point that the polymer matrix is melting, and the Pd particle growth is relatively fast as a result of the lifting of physical restrictions otherwise imposed by the solid polymer environment. Hence the relatively rapid development of catalytic activity followed by a decline as seen in Fig. 6.

The Pd-PABA system becomes active at temperatures well below the polymer melting point, melting not being required in order to expose the palladium, and the palladium particle growth is markedly slower.

Conclusions

The two palladium–polymer composites show a degree of similar behaviour in that both show a tendency for the palladium particles to grow when subjected to temperatures above room temperature and the palladium particles are of a similar size in the as-synthesized composites. Catalytic test reaction runs, however, demonstrate significant differences in the manner in which palladium is accessible to the gas phase. In the case of Pd-PPDA, the palladium appears to be accessible only if the polymer has melted, suggesting that the metal particles are otherwise largely buried within the polymer matrix. In the case of Pd-PABA, catalytic activity is observed at temperatures far below the polymer melting temperature and the interpretation is that the metal particles are exposed even at low temperatures, possibly as the result of the peculiar structure of the polymer. In both composites, palladium metal growth is seen, with relative growth being similar but at temperatures of 100°C for Pd-PPDA and 170°C for Pd-PABA. Palladium location and stability is therefore highly dependent on the nature of monomer used in the synthesis, and the nature of the monomer also dictates the detailed structure of the polymer matrix within the composite. Studies such as those described here add value in that they aid in our understanding of the detailed structure of nanometal–polymer composites and can assist in helping to assess the suitability of the materials in specific applications.

Financial assistance from the National Research Foundation is gratefully acknowledged.

Received 12 July. Accepted 3 November 2008.

1. Cowie J.M.G. (1991). *Polymers: Chemistry and Physics of Modern Materials,* 2nd edn. Chapman and Hall, New York.
2. Delmonte J. (1990). *Metal Polymer Composites.* Van Nostrand Reinhold, New York.
3. Kang E.T., Neoh K.G. and Tan K.L. (1998). Polyaniline: a polymer with many interesting intrinsic redox properties. *Prog. Polym. Sci.* **3**, 277–324.
4. Mallick K., Witcomb M.J., Dinsmore A. and Scurrell M.S. (2005). Polymerization of aniline by auric acid: formation of gold decorated polyaniline nanoballs. *Macromol. Rapid Commun.* **26**, 232–235.
5. Walton D.J. and Lorimer J.P. (2001). *Polymers.* Oxford University Press, Oxford.
6. Chaubey A., Pande K.K. and Malhotra B.D. (2003). Application of polyaniline/sol-gel derived tetraethylorthosilicate films to an amperometric lactate biosensor. *Anal. Sci.* **9**, 1477–1480.
7. Mallick K., Witcomb M.J., Dinsmore A. and Scurrell M.S. (2005). Fabrication of a metal nanoparticles and polymer nanofibers composite materials by an in-situ chemical synthetic route. *Langmuir* **21**, 7964–7967.
8. Mallick K., Witcomb M.J. and Scurrell M.S. (2006). *In-situ* synthesis of copper nanoparticles and poly (*o*-toluidine): a metal-polymer composite material. *Eur. Poly. J.* **42**, 670–675.
9. Wei Z., Zhnag Z. and Wan M. (2002). Formation mechanism of self-assembled polyaniline micro/nanotubes. *Langmuir* **18**, 917–921.
10. Gangopadhyay R. and De A. (2000). Conducting polymer nanocomposites: a brief overview. *Chem. Mater.* **12**, 608–622.
11. Mallick K., Witcomb M.J. and Scurrell M.S. (2006). Polyanaline stabilized highly dispersed gold nanoparticle: an *in situ* chemical synthesis route. *J. Mater. Sci.* **41**, 6189–6192.
12. Mallick K., Witcomb M.J. and Scurrell M.S. (2007). A novel synthesis route for a nanostructured gold-polymer soft composite material. *Phys. Stat. Sol. (RRL)* **1**, R1–R3.
13. Mallick K., Witcomb M.J. and Scurrell M.S. (2006). Palladium nanoparticles in poly (*o*-phenylenediamine): synthesis of a nanostructured 'metal-polymer' composite material. *J. Macromol. Sci: Pure Appl. Chem.* **43**, 1469–1476.
14. Mallick K., Witcomb M.J., Dinsmore A. and Scurrell M.S. (2006). Preparation of highly dispersed Pd-nanoparticles in poly-(*o*-aminophenol) needles: an 'Intimate composite material'. *J. Mater. Sci.* **41**, 1733–1737.
15. Mallick K., Witcomb M.J. and Scurrell M.S. (2006). Formation of palladium nanoparticles in poly (*o*-methoxyaniline) macromolecule fibers: an *in-situ* chemical synthesis method. *Eur. Phys. J. E* **19**, 149–154.
16. Mallick K., Witcomb M.J. and Scurrell M.S. (2005). Preparation and characterization of a conjugated polymer and copper nanoparticle composite material: A chemical synthesis route. *Mater. Sci. Engng B* **123**, 181–186.
17. Genies E.M., Boyle A., Lapowski M. and Tsintavis C. (1990). Polyaniline: a historical survey. *Synth. Methods* **36**, 139–182.
18. Lux F. (1994) Properties of electronically conductive polyaniline: a comparison between well-known literature data and some recent experimental findings. *Polymer* **35**, 2915–2936.
19. Mallick K., Witcomb M.J. and Scurrell M.S. (2006). Gold in polyaniline: recent trends. *Gold Bull.* **39**, 166–174.
20. Mallick K., Witcomb M.J. and Scurrell M.S. (2007). Palladium-polyaniline and palladium-polyaniline derivative composite materials. *Plat. Met. Rev.* **51**, 3–15.
21. Anderson J.R. (1975). *The Structure of Metallic Catalysts.* Academic Press, New York.